

Morphochemical characterization of *Chlamydomonas* during its blooming in a Mexican urban lake

Caracterización morfoquímica de *Chlamydomonas* durante un florecimiento en un lago urbano mexicano

José Luis Godínez-Ortega^{1*}, Laura Peralta-Soriano², Alfonso Lugo-Vázquez², Marco Antonio Escobar-Oliva³, María del Rosario Sánchez-Rodríguez² and María Guadalupe Oliva-Martínez²

Recibido: 30 de agosto de 2022.

Aceptado: 30 de noviembre de 2022.

Publicado: abril de 2023.

ABSTRACT

Background: Algal blooms have increased in frequency and intensity in recent decades. Excess nutrients of anthropogenic origin may be an essential factor that gives rise to these blooms. **Goals:** This work aimed to study an unusual bloom of the chlorophyte *Chlamydomonas* in an urban lake from a morphological and chemical approach. **Methods:** The study site was a small lake located in Cantera Oriente, Mexico City. Sampling was performed in February 2016 (the cold-dry season); environmental variables were measured *in situ*, and surface samples were obtained for organism abundance and chlorophyll-a concentration. An additional sample was freeze-dried for chemical analyses, and another sample was fixed in glutaraldehyde for ultrastructural studies by SEM, TEM, LM, and confocal microscopy, using the stain Nile red to detect the presence of intracellular lipids. **Results:** The results of morphological observations agreed with the characteristics of the description of *C. reinhardtii*. The bloom abundance values were high ($6.98 \times 10^5 \pm 1.37 \times 10^5$ cells mL^{-1}), confirmed by the high values of chlorophyll-a concentration ($5548 \pm 796 \mu\text{g L}^{-1}$). The carbohydrate:protein ratio of the cells (0.15) indicates high protein synthesis during the enormous algal proliferation. The low lipid content (6.5 %) is associated with the absence of intracellular lipid granules and may be related to the availability of nitrogen and phosphorus and high vegetative multiplication. *C. reinhardtii* synthesizes essential fatty acids, such as alpha-linolenic acid (Omega 3), a precursor of beneficial lipids in human cardiovascular and neurological health. **Conclusions:** The bloom consisted mainly of *Chlamydomonas reinhardtii* and it significantly correlated with the chlorophyll a concentration, indicating high photosynthetic capacity and active cell division. Linoleic acid (Omega 3), an important substance for human health, was present in the alga composition. A controlled culture of this alga could improve the Omega 3 concentration offering a biotechnological resource for the future.

Key Words: Chemical composition, Cytochemistry, SEM, TEM, Ultrastructure.

*Corresponding author:

José Luis Godínez Ortega: jlgo@unam.mx

To quote as:

López-Valdez, M. L., H. S. Espinosa-Pérez & A. L. báñez

Godínez-Ortega, J. L., L. Peralta-Soriano, A. Lugo-Vázquez, M. A. Escobar-Oliva, M. del R. Sánchez-Rodríguez & M. G. Oliva-Martínez. 2023. Morphochemical characterization of *Chlamydomonas* during its blooming in a Mexican urban lake. *Hidrobiológica* 33 (1): 1-14.

DOI:10.24275/um/itz/dcbs/hidro/2023v33n1/
Godínez

RESUMEN

Antecedentes: Los florecimientos algales han aumentado en frecuencia e intensidad en las últimas décadas. El exceso de nutrientes de origen antropogénico puede ser un factor esencial. **Objetivos:** Este trabajo tuvo como objetivo estudiar un florecimiento inusual de la clorofita *Chlamydomonas* en un lago urbano desde un enfoque morfológico y químico. **Métodos:** El sitio de estudio fue un pequeño lago somero ubicado en la Cantera Oriente, Ciudad de México. El muestreo se realizó en febrero de 2016 (época fría-seca); las variables ambientales se midieron *in situ* y se obtuvieron muestras de superficie para determinar la abundancia de organismos y la concentración de clorofila-a. Una muestra adicional se liofilizó para análisis químicos y otra muestra se fijó en glutaraldehído para estudios ultraestructurales mediante MEB, MET, ML y microscopía confocal, utilizando la tinción de rojo Nilo para detectar la presencia de lípidos intracelulares. **Resultados:** Los resultados de las observaciones morfológicas coincidieron con las características de la descripción de *C. reinhardtii*. Los valores de abundancia del florecimiento fueron altos ($6.98 \times 10^5 \pm 1.37 \times 10^5$ células mL^{-1}), lo cual se asocia con los altos valores de concentración de clorofila-a ($5548 \pm 796 \mu\text{g L}^{-1}$). La proporción de carbohidratos: proteínas de las células (0.15) indica una alta síntesis de proteínas durante la enorme proliferación de algas. El bajo contenido de lípidos (6.5 %) está asociado a la ausencia de gránulos de lípidos

intracelulares, posiblemente vinculado con la disponibilidad de nitrógeno y fósforo y a la alta multiplicación vegetativa. *C. reinhardtii* sintetiza ácidos grasos esenciales, como el ácido alfa-linolénico (Omega 3), un importante precursor de lípidos beneficiosos para la salud cardiovascular y neurológica humana. **Conclusiones:** Se concluye que el florecimiento estuvo constituido principalmente por *C. reinhardtii*, lo que se correlacionó significativamente con la abundancia y concentración de clorofila, indicando alta capacidad fotosintética y división celular activa. Se encontró la presencia en las algas del ácido linoléico (Omega 3), de importancia en la salud humana, que podría aumentar su concentración en un cultivo controlado y así ofrecer un recurso biotecnológico en el futuro.

Palabras clave: Citoquímica, Composición química, MEB, MET, Ultraestructura.

INTRODUCTION

Nutrient concentrations play a fundamental role in the growth of any phytoplankton population. So, the availability of nutrients is of great importance in determining the competitive capacity of algae (Baldia *et al.*, 2003). Algal blooms and their causes are different in temperate zones, where they occur in the warmer months and persist throughout the summer, in contrast to those occurring in tropical zones, where they can occur at any time of the year and persist for a few weeks (Mowe *et al.*, 2015). Excess nutrients, through anthropogenic inputs, are known to be a fundamental factor in the prevalence of these growths (Reynolds, 1984; Millie *et al.*, 1999). Often these growths, which are generally associated with cyanobacteria such as *Microcystis*, *Anabaena*, and *Cylindrospermopsis*, are detrimental (Mowe *et al.*, 2015). However, there are other uncommon blooms of euglenoids, diatoms, and *Chlamydomonas*; some authors classify the latter genus as forming “Harmful Algal Blooms” (HABs), as they frequently clog water purification filters (Kruskopf & Du Plessis, 2004). Species of the genus *Chlamydomonas*, unlike cyanobacteria, are not toxic in the strict sense, but they do produce certain allelopathic compounds that inhibit the growth of other microalgae and some zooplankton organisms (Barreiro & Hairston Jr. 2013). There are few records of blooms generated by *Chlamydomonas*, but proliferations have occurred mainly in Europe and Australia; for example, in backwaters of the Ruhr River in Germany (Herrman & Jüttner, 1977); in lagoons and canals in the Llobregat delta, Spain, in 1982 (Catalán, 1984); in the Vaal River, South Africa, in August 1992 (Pieterse & Janse van Vuuren, 1997); and in the Canning River estuary in Western Australia in 2001 (River Science, 2005). There is no record of these blooms in America, which motivated the interest in studying the bloom in a small water body in Mexico City.

Our planet is in the Anthropocene era, threatening biodiversity, and human life. Studying fast-growing, oxygen-producing, nutraceuticals and biodiesel producing microalgae could help combat climate change and greenhouse gases. *Chlamydomonas reinhardtii* is a species that can be manipulated in artificial cultivation to produce high-value products such as biodiesel, nutraceutical, food, and medicinal substances. In addition, this alga has biotechnological potential since it grows in small spaces, without competition for space, by taking advantage of arid soils for its cultivation, as well as sunlight, which together with the physical and chemical conditions of the water could promote rapid and optimal growth (Scranton *et al.*, 2015).

This research's objective was to determine the species forming the bloom observed in 2016 in the North Lake of the Cantera Oriente and its morphological and chemical characterization.

MATERIAL AND METHODS

Study area. The bloom occurred in one of the four lakes located within the Cantera Oriente (CO) ($19^{\circ}19'08''$ N and $99^{\circ}10'21''$ W), which is part of the Reserva Ecológica del Pedregal de San Ángel (REPSA), Mexico City, with an area of 206 000 m². The Cantera Oriente arose due to the extraction of volcanic rock (basalt), a concession of the UNAM to the Mexico City Asphalt Plant from 1970 to 1994; two years later, the Cantera Oriente was incorporated into the REPSA (Lot, 2007).

The climate of the Cantera Oriente is temperate sub-humid, with summer rains and dry winters. The average annual precipitation was 833 mm; the average annual temperature was 15.6 °C; the prevailing winds came from the N and NNE, and the altitude was 2559 m.a.s.l. The lakes in this area are classified as high-altitude aquatic systems; however, they are tropical lakes, considering their latitude. These water bodies are shallow, and despite sharing the same supply source, they present different environmental conditions, especially regarding their trophic status. The water bodies of the Cantera Oriente were characterized as eutrophic-hypertrophic (Lugo-Vázquez *et al.*, 2017).

Due to its geographic location, the lake under study was named Lago Norte (LN), with a maximum length of 198 m and 77 m in its widest portion, with an approximate area of 5450 m². It has a narrow channel (~10 m wide x ~159 m long) that is not easy to access, and it is presumed that water flows from the channel and runs into the water table. In the southern region, a gate links the LN to another larger aquatic system, Lago Centro (LC), which feeds water to the LN along with other channels from springs in the aquifer. The LN is a shallow body with a maximum depth of 1.20 m and is surrounded by arboreal vegetation, shrubs, and aquatic plants rooted in some parts of the littoral zone (*Typha latifolia* L.), with *Stuckenia pectinata* (L.) Börner predominant in the channels and free-floating *Lemna gibba* L. (Lot, 2007; Cuevas-Madrid *et al.*, 2020).

Light and Confocal Microscopy. Sampling was conducted on February 23, 2016, corresponding to the cold-dry season. Direct samples were taken from the surface layer (5 cm) to determine the morphological characteristics of the microalgae. A Zeiss light microscope (LM), model 1206 S09432 (Germany) was used, and images were taken with a Canon PowerShot G6 digital camera (Japan). For the confocal microscopy study, cells were fixed using 2% glutaraldehyde and re-suspended in a phosphate solution (pH 7.2-7.4, 0.1 M) (Mohan, 2006) and stained with Nile red (Sigma, Saint Louis, USA) at a final concentration of 2.5 µg mL⁻¹ (from a stock solution of 50 µg mL⁻¹ in methanol), followed by a 10 min incubation in the dark (Greenspan *et al.*, 1985; Siaut *et al.*, 2011). Images were captured using a Zeiss LSM (Germany) 800 confocal microscope with DIC optics and a plan-apo-63X oil immersion objective. Post-acquisition image management was performed using Zen software (Carl Zeiss, Germany). Cells were stained with the Nile red and visualized with 488 nm argon laser-generated fluorescence combined with a 560 to 615 nm filter to detect neutral lipids; for the combined Chlorophyll-Nile red fluorescence of polar lipids, a 647 to 753 nm filter was used.

Electron Microscopy. For scanning electron microscopy (SEM), the sample was fixed in glutaraldehyde (2%), washed with distilled water, and dehydrated in alcohols gradually (10-100 %), brought to a critical point (EMITECH K 850), and then mounted in aluminum sample holders on carbon tape and metalized with gold for 2 min (QUORUM Q1510 ES). The samples were then observed in SEM (Hitachi SU1510, Hitachi, Japan), at a working distance of 15 mm and a voltage of 15 kV.

For transmission electron microscopy (TEM), the sample was fixed in 2% glutaraldehyde in phosphate buffer (pH 7.2-7.4) for two hours at 4°C. Cells were centrifuged at 500 g (1500 rpm) for 10 min. Post-fixation was performed with osmium tetroxide (1%) for 1 min. They were dehydrated with increasing series (10-100%) of ethyl alcohol at 4°C and embedded in epoxy resin (EPON®). Ultra-sections were 90 nm and contrasted with uranyl acetate (0.5 % to 3 %) and lead citrate (3%). Samples were observed and imaged on a TEM (JEOL, Model JEM1200 EX II, Tokyo, Japan) (Siaut *et al.*, 2011), with a resolution of 0.15 nm, an accelerating voltage of 60 to 120 kV, and a magnification of 50x to 500,000x (Toledo *et al.*, 2016). The service of the Imaging Unit of the Institute of Cell Physiology, UNAM, was used.

Liquid samples and permanent preparations were incorporated with their identification number (NI: 2481, 2486, 2491, 2492, 2510, 2581) in the National Herbarium of Mexico (MEXU).

Chemical analyses. An abundant filtered surface water sample (10L) of *Chlamydomonas* was lyophilized for chemical analyses. According to the methods proposed by AOAC International (2019), lipid content was determined by Soxhlet extraction (AOAC:920.85), nitrogen by Kjeldahl method (AOAC:978.04), protein percentage was calculated as the percentage of nitrogen multiplied by the factor 6.25, and ash content by combustion in a muffle at 550 °C. (AOAC:930.05). Total carbohydrate content was determined by difference [100 - (%moisture + %ash + %fat + %protein + dietary fiber)] (Pehrsson *et al.*, 2015). Dietary fiber (AOAC:992.16) was quantified with enzymatic (α -amylase 5%) and gravimetric autoclave treatment, and the residue was weighed to determine the ratio. Moisture was determined by vacuum drying (3 h) at a constant temperature (70°C) (AOAC: 925.04).

A homogenized sample of the algae was extracted using the methanol/dichloromethane method (2v/1v) to ascertain the fatty acid composition. Methyl esters (FAMEs) were prepared according to AOAC Method (AOAC:996.06). Fatty acids determination was performed with an FID gas chromatograph (Scion Model 436-GC, Compass CDS Software Version 3.0.2.144), equipped with a flame ionization detector and a capillary column (Thermo Scientific TG-Polar 105 m*0.25 mm * 0.2 μ m). Ultrahigh purity nitrogen was used as the carrier gas, and the method used was: 100 °C for 4 min, a gradient of 3 °C min⁻¹ to reach 240 °C for 15 min. The chromatograms were identified with a FAME mixture standard's retention times and correction factors (CRM47885, Supelco).

The catalytic combustion technique analyzed the percentage of total de carbon at 900°C in a Shimadzu brand equipment model TOC-L SSM-5000A (Shimadzu Corp., Kyoto, Japan; Jha *et al.*, 2014). For total nitrogen, digestion with H₂SO₄ and vapor entrainment titration was carried out. Total phosphorus was quantified by molybdate yellow complex colorimetry (AOAC: 995.11).

Cell density, chlorophyll, and environmental parameters. Direct samples were taken in triplicate from the surface using Falcon tubes

(50 mL). From each sample, three counts were performed to obtain cell density (n=9), using a Neubauer camera and 40X magnification.

These same samples were used to quantify chlorophyll-a concentration by performing triplicate measurements (n=9). A known volume (1 ml) was filtered, using Whatman GF/F fiberglass filters, according to the cold extraction method (4°C) with 90% acetone, using a Turner Designs model 10-AU fluorometer (Arar & Collins, 1997).

The main environmental parameters of the water column were measured *in situ* with conventional methods, using a YSI model 85 multiprobe and pH with a Conductronic model pH10 field potentiometer.

Chemical digestion of the organic matter was previously carried out with potassium persulfate solution (100 ml 0.375 N NaOH, 5 g of Potassium Persulfate, and 3 g of Boric Acid) under alkaline conditions using Valderrama (1981) method to quantify total phosphorus and nitrogen. Then, total nitrogen was measured as N-NO₃⁻¹ and total phosphorus as P-PO₄³⁺. The concentrations of ammoniacal nitrogen N-NH₃, nitrogen as nitrites (N-NO₂) and nitrogen as nitrates (N-NO₃), and dissolved reactive phosphorus (P-PO₄) were also measured. Dissolved inorganic nitrogen (DIN) was calculated from the above data. Bicarbonate concentration was calculated using the proportion between phenolphthalein and methyl orange alkalinity and transforming HCO₃⁻¹ concentration as mg L⁻¹ as CaCO₃ in HCO₃⁻ (mg L⁻¹). Concentrations of Ca²⁺ and Mg²⁺ was calculated using the total and calcium hardness data. Methods described by APHA *et al.* (1985) were used.

Statistical analyses. A linear regression analysis between cell densities and chlorophyll-a concentration was performed using the PAST 4.06 package (Hammer *et al.*, 2001). Both data set were previously transformed to log₁₀.

RESULTS

Taxonomy and morphology. *Chlamydomonas* is classified within the Phylum Chlorophyta, Class Chlorophyceae, Order Chlamydomonadales, and Family Chlamydomonadaceae. It is a unicellular alga that is distinguished into different subgenera depending on the position of the pyrenoid. In the case of the Cantera Oriente bloom, the alga has a basal pyrenoid that includes it in the subgenus Euchlamydomonas and the Bivacuolatae group because it presents two contractile vacuoles apically. Blooming species was determined as *Chlamydomonas reinhardtii* P.A. Dangeard, 1888 (Fig. 1B).

Light microscopy (vegetative cells). Cells are solitary, free, broadly ovoid, 8-30 μ m long, and 7-22 μ m in diameter (Fig. 2A, B). Cup-shaped chloroplast and single pyrenoid, with a halo of starch grains, located in the lower part of the chloroplast (Fig. 2B). Two flagella of equal length or slightly shorter than the cell body emerges from the cell's anterior region without a papilla (Fig. 2C). The protoplast is observed separately from the cell wall (Fig. 2B, E). The base of the cell is circular 7-23 μ m; in this view, the pyrenoid is observed to be large and well-positioned in the central part (Fig. 2D).

Scanning and transmission electron microscopy (vegetative cells). The cells are ovoid or truncated pear-shaped, without a papilla in the longitudinal section (Fig. 3A). Remnants of the flagellar base are visible in the anterior region, just above the vacuoles. Mitochondria were located near the anterior-lateral cytoplasm under two contractile vacuoles,

the stigma and laterally the chloroplast with thylakoids (Fig. 3B). The nucleus is spherical (Fig. 3A, B) and situated slightly above the medial region. The cup-shaped chloroplast contains a pyrenoid in the posterior region (Fig. 3A, C). In the basal view, the pyrenoid is centrally located (Fig. 3C) with a white halo containing starch (Fig. 3D); tubular structures are observed in the centre of the pyrenoid (Fig. 3C, D). The relatively large stigma is located above the mitochondrion in the lateral-anterior region (Fig. 3B) above the mitochondrion.

In SEM, the cells in the lateral view are flattened pear-shaped with a smooth wall and a vestige of the flagellar apparatus in anterior position (Fig. 3E); in the basal view, the cells are circular and smooth-walled (Fig. 3F).

Table 1 summarizes the morphological characteristics of *C. reinhardtii*, including habitat and geographic distribution. The species under study is compared with four other microalgal species. *C. reinhardtii* is the only species (Table 1) to be ovoid; in ML, its anterior region is ellip-

soid, with a large basal pyrenoid and a mature thick-walled zygospore with anastomosing thickenings. The habitat is freshwater with a wide or cosmopolitan distribution, except for arctic regions (Table 1). Some organisms were mixed with *Chlamydomonas* with very low abundance (*Desmodesmus abundans* (Kirchner) E.H. Hegewald, diatoms, and some rotifers).

Light and electron microscopy (reproductive cells). Figures 4A-C show different stages of zygospores (juvenile to mature), with a diameter that ranged from 20 to 33 μm . Using Nile red staining and fluorescence in LM, bright yellow lipid droplets are distinguishable within the zygospore (Fig. 4A). Figures 4A and 4B show a thick and smooth outer wall and a thin inner membrane; under the wall, there are wavy or honeycombed ornamentations (Fig. 4A, B); the cytoplasm had a positive reaction to Lugol due to the abundance of starch; other developing reproductive cells without a reticulated wall are also observed (Fig. 4B). In SEM, an anastomosing reticulum protruding from the hexagonal-shaped outer layer is observed (Fig. 4C). In TEM, a well-formed two layers'

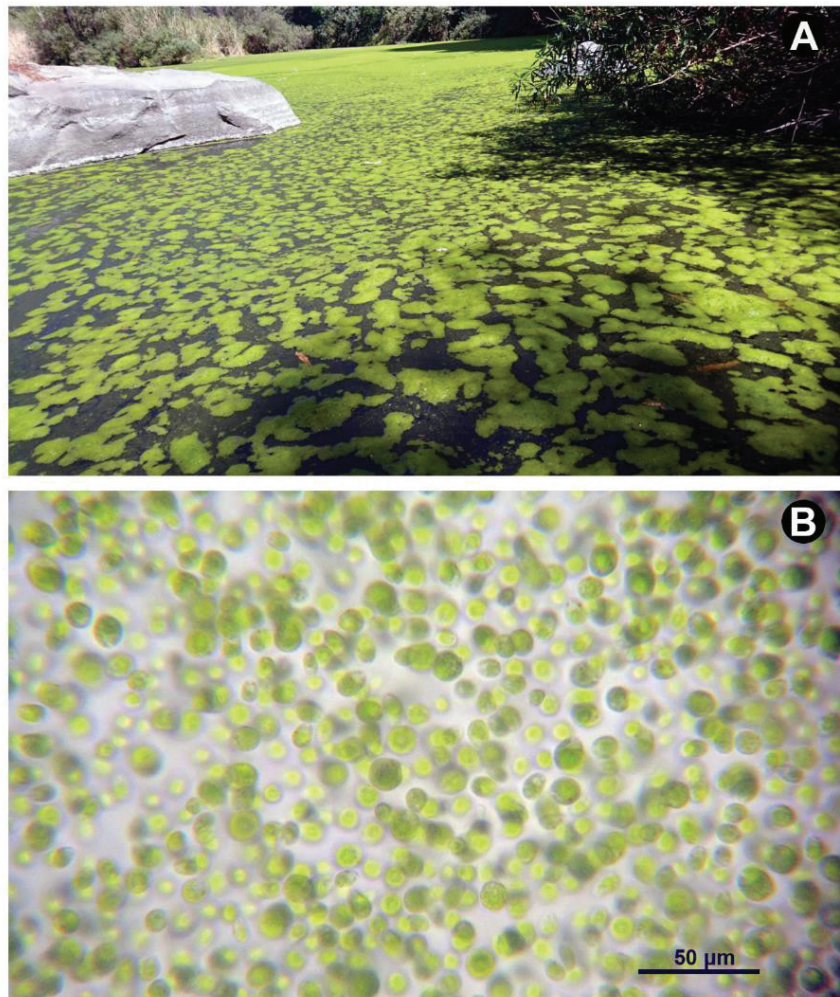


Figure 1. Blooming of *Chlamydomonas* in the Cantera Oriente lake (February 23, 2016). (A) Appearance of the algae on the surface of the lake. (B) Massive appearance of the algae in microscopic view.

wall is observed; a darker outer one and a more homogeneous inner one; undulations in the outer layer can be distinguished that coincide with the anastomosed reticular thickenings; inside the cell, a homogeneous cytoplasm without the presence of organelles is observed, with many white granules, which probably contained reserve substances (Fig. 4D).

Chemical analyses. The chemical composition of a wild population of *C. reinhardtii* during bloom in February 2016 is presented for the first time and compared with other microalgae grown under laboratory conditions (Table 2). Globally, chemically studied microalgae are represented by only ten species; however, based on these studies, we observe that the protein values of *C. reinhardtii* are in the concentration range

of these microalgae (11-77 %, Barka & Blecker, 2016); carbohydrates (10-57%, Becker, 2004) and lipids (4-22 %, Becker, 2004). Currently, considering algae as an essential protein source is based not only on its high concentration but also on the set of other chemicals such as carbohydrates, fats, antioxidants, vitamins, etc. (Becker, 2004). The carbohydrate:protein ratio was low (0.15), while the lipid:protein ratio was slightly higher (0.3).

Fatty acid percentages are presented in Table 3. In *C. reinhardtii* from the Cantera Oriente, saturated fatty acids (SAFA, C16:0, 3.7%) were in higher proportion than monounsaturated (MUFA, 0.8%) and polyunsaturated (PUFA, 0.2-0.6 %). Palmitic acid (3.7%) stands out, followed by oleic acid (0.8%) and then linoleic acid (0.6%).

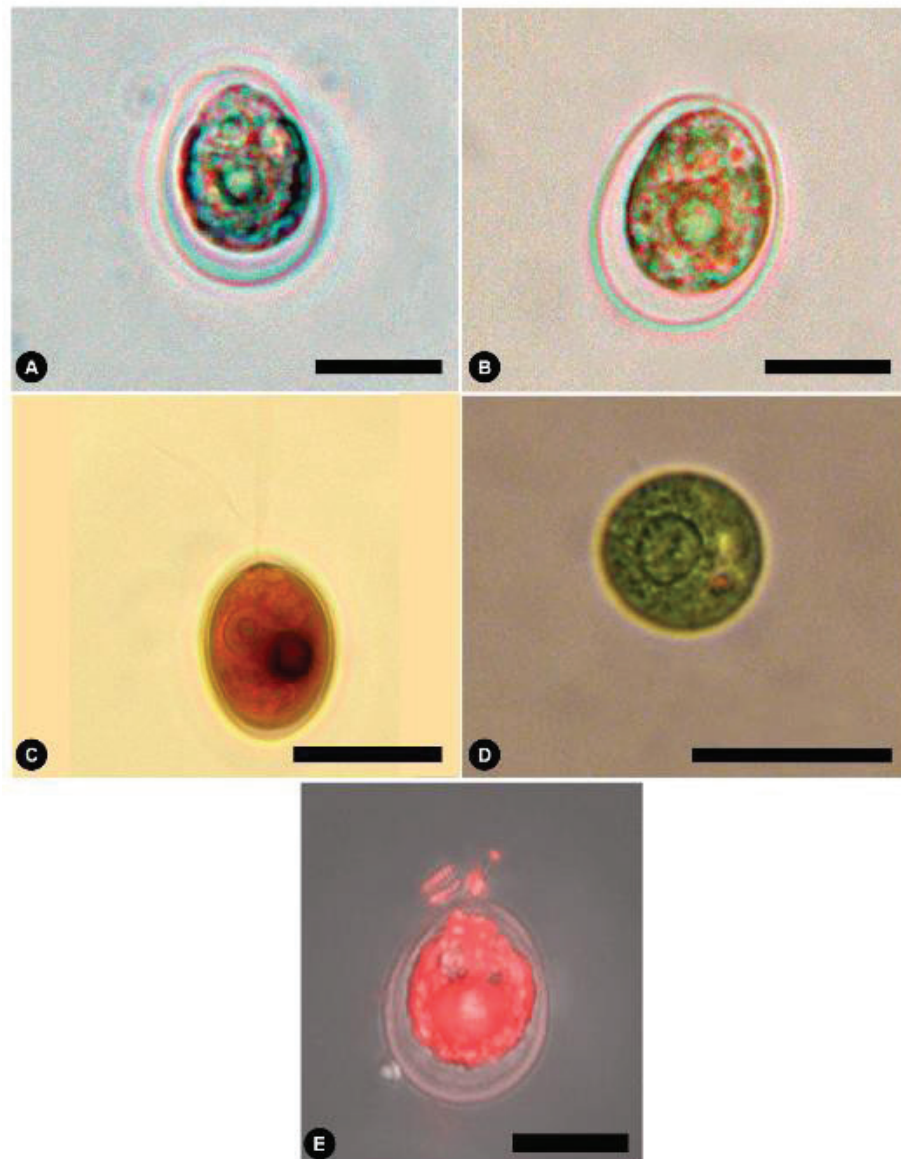


Figure 2. *Chlamydomonas reinhardtii* from the Cantera Oriente bloom. (A-B) Light microscopic views of the alga. (C) View of cell with two flagella, stained with Lugol. (D) Basal view of living alga, central pyrenoid is observed. (E) Cell with Nile red staining in fluorescence. Scale bars represent: A-C, 5 μ m; D, 10 μ m; E, 20 μ m.

Table 1. Comparison of principal morphological features of *Chlamydomonas reinhardtii* and other species.

Feature	<i>C. reinhardtii</i>	<i>C. ehrenbergii</i>	<i>C. snowiae</i>	<i>C. globosa</i>	<i>C. incerta</i>
Cell shape	ovoid	pear-shaped	piriformis	spherical	spherical - broadly ellipsoid
Cell size	7-22 x 8-30 μm	14-26 μm	4-18 x 10-24 μm	5-7.8 μm	8-9.5 x 9.7-12.4 μm
Anterior shape	ovoid	slightly apiculate or narrow	conical	rounded	rounded
Posterior shape	rounded	rounded	rounded, basally thickened	rounded, slightly thickened	rounded
Flagella length	slightly shorter as the cell	1½-2 times body length	slightly shorter as the cell	1½ times longer as the cell	slightly longer as the cell
Position of the nucleus	above the middle of the cell	in the middle of the cell	above the middle of the cell	in the middle of the cell	above the middle of the cell
Contractile vauoles	2 apical	2 apical	1 apical	1 apical	2 apical
Cell wall papilla	no	yes	conical	no	no
Cell wall	smooth	smooth	with a series of fine lateral striations	smooth	smooth
Chloroplast shape	cup-shaped	cup-shaped, thickened at the base	cup-shaped	cup-shaped	cup-shaped
Pyrenoid	1, round-slightly	1 small, round	1	small, round-slightly ellipsoid	medium, round-slightly ellipsoid
Position of the pyrenoid	basal	eccentric	basal	basal	basal
Eyespot	1 elliptic	1 elliptic	1 or more	1 dot-like	elliptic
Position of the eyespot	anterior side	median or antero sider	median or antero side	median or anterior side	anterior side
Plasma membrane	oftenly withdrawn from the cell wall	protoplasm sometimes detached from cell wall	no	no	no
Zygospor wall	smooth with hexagonal wall thickenings	thick, pitted, and sculpted outer layer (fine warts).	unknown	unknown	unknown
Zygospor size	21.1-33 μm	12-16 μm			
Habitat*	freshwater	freshwater	freshwater/terrestrial	freshwater/terrestrial	freshwater
Distribution*	Europe, North America, Mexico, South America, Middle East, South-west Asia, Asia, Australia, New Zealand	Africa, Europe, Middle East, North America, South America, South-west Asia	Arctic, Europe, North America, South America, Middle East, South-west Asia, Asia, Australia, New Zealand	Europe, North America, South America, Middle East, South-west Asia, Asia, Australia, New Zealand	Europe, North America, Caribbean Islands, Middle East, Asia
Reference	This study	Pascher (1927); John et al., (2011)	John et al. (2011)	John et al. (2011); Pröschold et al. (2018)	Pröschold et al. (2018)

* Guiry & Guiry (2021).

Neutral lipids (triacylglycerols) were observed in reproductive cells (zygospores), using the Nile red fluorescence technique, like bright yellow circular droplets (Fig. 4A); conversely, vegetative cells showed no reaction to the Nile red (Fig. 2E). Ash values are well within the wide range of microalgae (8-40%, Table 2) (Becker, 2004).

Element contents (C, N, P) are presented in Table 4. Algal carbon (37.37%) was higher than nitrogen (3.26%) and phosphorus (0.44%). The C/N ratio was higher (11.46%) than the N/P ratio (7.40%), and the C/P ratio was high (84.93%).

Cell density, chlorophyll, and environmental conditions. Cell abundance or cell density values were high ($6.98 \times 10^5 \pm 1.37 \times 10^5$ cells mL^{-1}), which is confirmed by extreme values of chlorophyll-a concentration ($5548 \pm 796 \mu\text{g L}^{-1}$) (Fig. 5). Regression analysis between the log of *Chlamydomonas* cell abundance values and the log of chlorophyll a concentration was significant ($r^2 = 0.9362$, $p < 0.001$). Residuals have a normal distribution (Shapiro-Wilks test 0.8995, $p = 0.272$), and the Durbin-Watson test (2.9995, $p = 0.95$) indicated no significative autocorrelation in y values residuals. The Breush-Pagan statistic (1.4645) corroborates the homoskedasticity ($p = 0.226$) of residuals. Data used for regression analysis were obtained directly from field samples. This fact explained the not-so-high r^2 value obtained. Several other phytoplankton species could be present in variable abundances in the samples, increasing the chlorophyll concentrations and reducing the relationship between both variables.

Photosynthetically active light was recorded in the study period (January-March) in a range of 0.003-2361 $\mu\text{mol photon m}^2 \text{s}^{-1}$ (Fig. 6); an increase was observed towards March.

The environmental conditions during the bloom do not allow us to identify the variables promoting the bloom. The blooming occurred during the coldest period of the year, with temperatures around 15 °C. Several variables showed a slight decrease during bloom, such as the concentration of bicarbonate (39 to 34 mg L^{-1}), calcium (37 to 34 mg L^{-1}), and nitrates (5.9 to 5.4 mg L^{-1}). Others also increased slightly, such as dissolved reactive phosphorus (0.11 to 0.15 mg L^{-1}), nitrogen as nitrite, N-NO_2 (0.013 to 0.021 mg L^{-1}), magnesium (26 to 29 mg L^{-1}) and conductivity (389 to 419 $\mu\text{S cm}^{-1}$). The N-NH_3 concentration doubled (0.05 to 0.10 mg L^{-1}). Finally, variables whose values increased probably due to the bloom effect, such as D.O. (8.1 to 8.8 mg L^{-1}) and pH (6.7 to 7.3).

DISCUSSION

Because of the basal position of the pyrenoid and a cup-shaped chloroplast in both ML and TEM microscopy, this alga is included in the subgenus Euchlamydomonas. The specific diagnosis was *C. reinhardtii*, based on cells with two apically contractile vacuoles oriented perpendicular to the plane of the two flagella (Bivacuolatae group); the cell has a smooth chloroplast, without divisions or lobules; the cells are neither hemispherical nor flattened, the stigma is present, the cell is broadly ovate and has no papilla. It is closely related to *C. ehrenbergii*, due to its size, shape, ultracellular arrangement, and the presence of two vacuoles below the flagellar apparatus; however, *C. ehrenbergii* is apiculate in its anterior region and has a papilla, as does *C. snowiae*. It was observed that the species under study has a plasma membrane that separates from the cell wall, which is not the case with *C. globosa*, *C. snowiae* and *C. incerta* (Table 1); in addition, *C. globosa* is smaller (5-7.8 μm), spherical, and has only one contractile vacuole. *C. incerta* differs from *C. reinhardtii* by containing flagella larger than its cell and is spherical to ellipsoidal (Table 1). The zygospores of *C. reinhardtii* differ from *C. ehrenbergii* in size; the outer, mature cell wall has anastomosing thickening in *C. reinhardtii* and warty in *C. ehrenbergii*. The zygospore seen in TEM sections presents a two-layered cell wall, which is very similar to those of Heimerl *et al.* (2018), who studied the same species.

Regarding the chemical composition of the blooming algae, it had a moderate protein content (19.2%). Differences are observed in comparing the protein, carbohydrate, and lipid content of *C. reinhardtii* with other microalgae; the cyanobacterium *Limnospira maxima* had the highest protein concentration (50.4%), as did other green algae such as *Chlorella* sp. (45.3%). The cultivated strain of *C. reinhardtii* also had a higher protein content (46.9%). The Mexican strain presented a low amount of carbohydrates (2.9%) compared to the cultured microalgae *Porphyridium cruentum* (72.6-77.7%), *C. reinhardtii* (23.0%), *Chlorella* sp. (28.0%), and *Tetradesmus obliquus* (68.8%). The lipids of *C. reinhardtii* (6.5%) from the Cantera Oriente had similar values to *Anabaena cylindrica* (4-7%) and were in higher proportion than *Dunaliella salina* (3.0%); but their values were lower than cultured *C. reinhardtii* (24.7%), *Tetradesmus obliquus* (11.0%), and *Chlorella* sp. (16.1%). The analysis showed a high proportion of ash (25.5%) compared to *Chlorella* (9.3%) and *Limnospira* (11.4%). In general, the species under study

Tabla 2. Comparative chemical analysis of *Chlamydomonas reinhardtii*.

Relative contents (%)	Phylum	Origin	Protein	Carbohydrate	Lipid	Ash	Reference
<i>Chlamydomonas reinhardtii</i>	Chlorophyta	*	19.2	2.9	6.55	25.5	This study
<i>Chlamydomonas reinhardtii</i>	Chlorophyta	**	46.9	23.0	24.7	4.8	Darwish <i>et al.</i> (2020)
<i>Chlorella</i> sp.	Chlorophyta	**	45.3	28.0	16.1	9.3	Darwish <i>et al.</i> (2020)
<i>Dunaliella salina</i>	Chlorophyta	**	22.4	21.7	3.0	52.8	El-Baz <i>et al.</i> (2017)
<i>Tetradesmus obliquus</i>	Chlorophyta	**	19.0	68.8	11.0	1.1	Oliveira <i>et al.</i> (2020)
<i>Limnospira maxima</i>	Cyanobacteria	**	50.4	23.0	14.1	11.4	Darwish <i>et al.</i> (2020)
<i>Anabaena cylindrica</i>	Cyanobacteria	**	43-56	25-30	4-7	5-10	Becker (2004); Allen & Arnon (1955)
<i>Synechococcus</i> sp.	Cyanobacteria	**	63	15	11		Becker (2004)
<i>Porphyridium cruentum</i>	Rhodophyta	**	0.07-0.34	72.6-77.7	undetected	14-32	Agustina <i>et al.</i> (2020)

* Wild algae; ** Cultivation conditions

presented marked poverty of fatty acids compared to other species (Table 3); however, myristic acid (0.9 %), linolenic acid (0.8 %), arachidonic acid (0.1 %) of *D. salina*, and α -linolenic acid (Omega-3) of *L. maxima* had similar values with *C. reinhardtii* from the Cantera Oriente. In contrast, linolenic acid from *Chlorella* sp. (31.4 %), *L. maxima* (19.0 %) y *C. reinhardtii* (12.1 %), presented higher concentrations than in wild *C. reinhardtii* (0.6 %). However, it must be considered that the algae under study are from wild or natural conditions, and the other algae, such as *Chlorella*, *Limnospira*, *Tetradesmus*, and *Dunaliella* (Tables 2, 3), come from controlled cultures that could promote an increase in these substances.

The absence of intracellular lipid bodies through the Nile red reaction and fluorescence (Fig. 2E) and the absence of grey nodules (fat droplets) in transmission microscopy photography lateral and basal view respectively (Fig. 3A, C) confirmed that triacylglycerols (TAGs) were ab-

sent. In contrast, both storage entities (starch granules and lipid bodies) were found abundant in 30-day cultured cells in laboratory cultures (Darwish *et al.*, 2020). It is well known that lipid accumulation as TAG in microalgae increases as cells age, usually due to intracellular nutrient (nitrate) consumption during stationary growth and is accompanied by a cessation in cell division. Salas-Montantes *et al.* (2018) points out that the biosynthesis of triacylglycerols from algae is of growing interest for biodiesel production. They found that changes in gene expression in the *Chlamydomonas reinhardtii* strain overexpressing a transcription factor in response to nutrient deficiency increased its total fatty acid content (17.02%) in a medium without nitrogen. The most common fatty acids found were palmitic, oleic, and linoleic. Ochoa-Alfaro *et al.* (2019) observed an increase in cell growth, chlorophyll, and lipids concentration at pH values of 7.8. The authors point out that combining different strategies can help to obtain a high-value product (Hernández-Torres *et al.*, 2016).

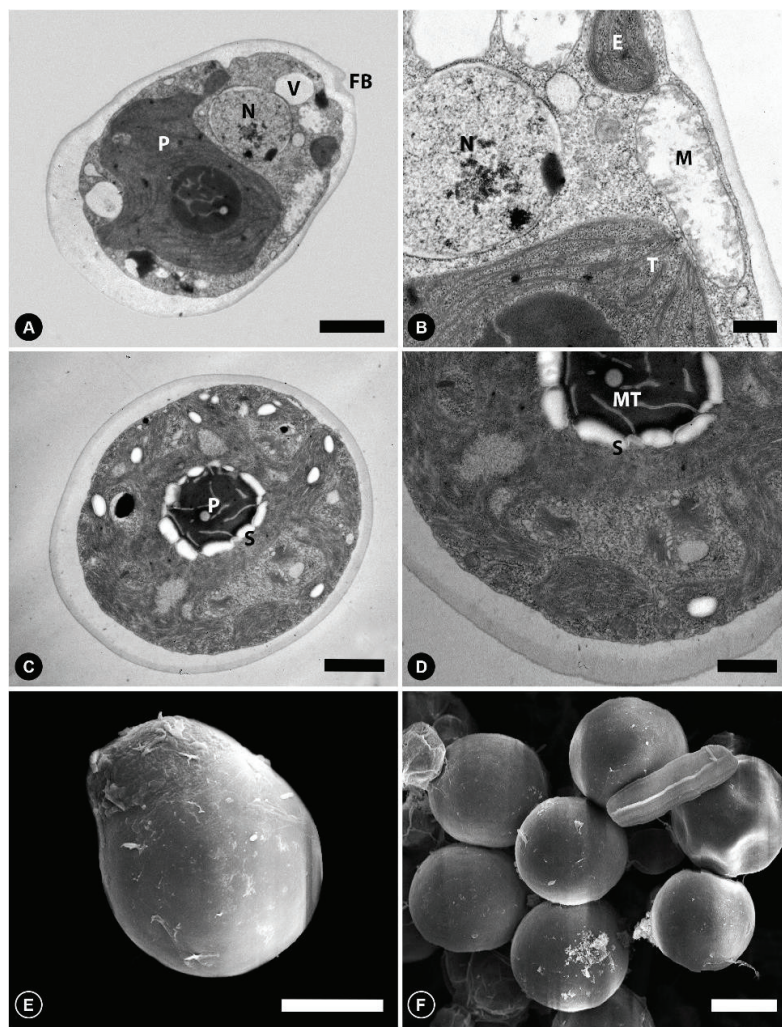


Figure 3. TEM and SEM micrographs of *Chlamydomonas reinhardtii*. (A) TEM overview of a complete cell. (B) Detail in TEM with mitochondria and stigma. (C) TEM basal view, pyrenoid with starch granules. (D) TEM detail with a pyrenoid with microtubules. (E) SEM view of complete cell and a vestige of the anterior flagellum. (F) Basal view in SEM. N, nucleus; CP, chloroplast; V, vacuoles; FB, flagellar base; M, mitochondrion; T, thylakoids; P, pyrenoid; S, starch; MT, microtubules; E, stigma. Scale bars represent: A, C, 2 μ m; B, 0.5 μ m; D, 1 μ m; E, F, 10 μ m.

Tabla 3. Fatty acid profile of *Chlamydomonas reinhardtii* (%).

Fatty acids	Common name	<i>C. reinhardtii</i> * This study	<i>C. reinhardtii</i> ** Darwish <i>et al.</i> (2020)	<i>C. reinhardtii</i> ** Ochoa-Alfaro <i>et al.</i> (2019) (pH 7.8)	<i>Tetraedesmus obliquus</i> ** Becker (2004)	<i>Chlorella</i> sp.** Darwish <i>et al.</i> (2020)	<i>Dunaliella salina</i> ** El-Baz <i>et al.</i> (2017)	<i>Limnospira máxima</i> ** Darwish <i>et al.</i> (2020)
C12:0	Lauric acid	ND	-	-	0.3	-	-	-
C14:0	Myristic acid	0.7	-	0.43	0.6	-	0.9	-
C16:0	Palmitic acid	3.7	23.8	28	16	22.2	6.0	57.9
C16:1ω7	Palmitoleic acid	ND	27.0	-	8	13.0	0.8	0.1
C18:0	Stearic acid	ND	23.0	4.4	0.3	28.0	31.5	1.5
C18:1ω7	Oleic acid	0.8	-	4.89	8	-	5.9	-
C18:2ω6	Linolenic acid	0.6	3.8	12.1	6	31.4	0.8	19.0
C18:3ω3	α-linolenic acid Omega 3	0.2	4.1	9.77	28	23.4	-	0.1
C20:0	Arachidic acid	0.5	-	-	-	-	0.1	-
Reference		This study	Darwish <i>et al.</i> (2020)	Ochoa-Alfaro <i>et al.</i> (2019) (pH 7.8)	Becker (2004)	Darwish <i>et al.</i> (2020)	El-Baz <i>et al.</i> (2017)	Darwish <i>et al.</i> (2020)

* Wild; ** Cultivation condition

This reflects that the Cantera Oriente bloom was not in a stationary phase, but in a state of exponential growth and cell division, efficiently utilizing nutrients (Khozin-Goldberg & Cohen, 2006; Moellering & Ben-

ning, 2010). Lipid droplets were only observed in the resistance structures (zygospores), meaning that these structures require lipid storage to enter dormancy. Zygospores were very scarce.

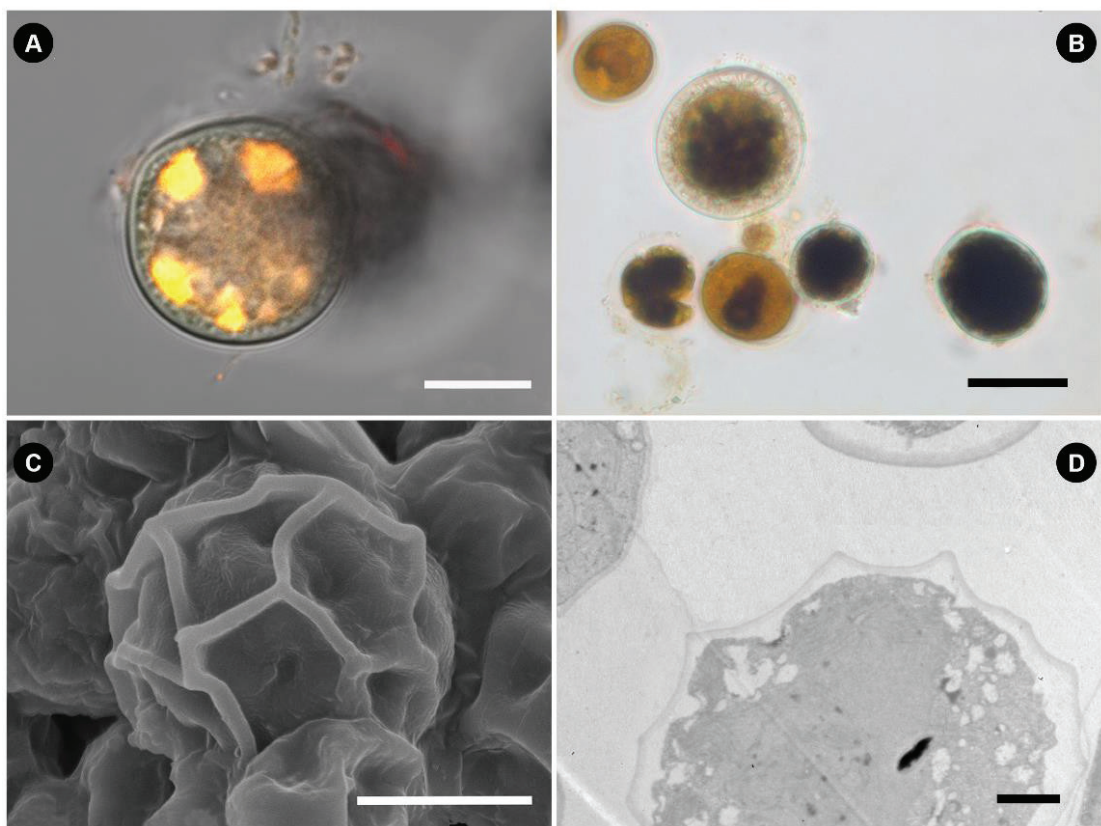


Figure 4. - Zygospores of *Chlamydomonas reinhardtii* from the Cantera Oriente bloom. (A) Bright yellow lipid granules with Nile red staining in fluorescence. (B) Zygospores at different stages of development with Lugol stain, (C) Zygospore in SEM; (D) Zygospore in TEM. Scale bars represent: A-C, 10 μ m; D, 2 μ m.

Table 4. Nitrogen, phosphorous and carbon content of *Chlamydomonas reinhardtii* bloom.

Element	%	SD
N	3.26	
P	0.44	
C	37.37	0.44
C/N	11.46	0.13
N/P	7.40	
C/P	84.93	

Chlorophyll-a concentration was high in the bloom ($5548 \mu\text{g L}^{-1}$) compared to the natural concentration in the water column in January and March (17.05 and $13.38 \mu\text{g L}^{-1}$). Chlorophyll-a concentration is an indicator of algal biomass. It is related to the fact that during the bloom,

there is more protein production because the carbohydrate:protein ratio (0.15) was very similar to that reported in an experimental culture of *C. reinhardtii* (0.13 to 1.2) during the exponential phase (Dean et al., 2008). The biochemical relationship of carbon, nitrogen, and phosphorus content to producing organic compounds is a necessary and survival relationship (Moellering & Benning, 2010). The N:P ratio is around 16 when in a stoichiometric equilibrium state, while in the Cantera Oriente an N:P ratio of 43 was obtained which exceeded the Redfield ratio, indicating a low proportion of phosphorus (Granéli et al., 2008; Smith et al., 2017). The three primary fatty acids (Omega-3) contained in the membranes are alpha-linolenic acid (ALA), eicosapentaenoic acid (EPA), and docosahexaenoic acid (DHA). Given the presence in the alga under study of ALA (Table 3) in chloroplast membrane glycerolipids, its importance in maintaining membrane fluidity at optimal growth temperatures (Hixson & Arts, 2016) and preventing membrane rigidity at suboptimal low temperatures can be assumed (Mansilla et al., 2004). Phosphate availability in the plant cell is often limited, and galactolipids predominate in plants and algae to reduce algal dependence on phosphate (Kalisch et al., 2016). It has been seen that with

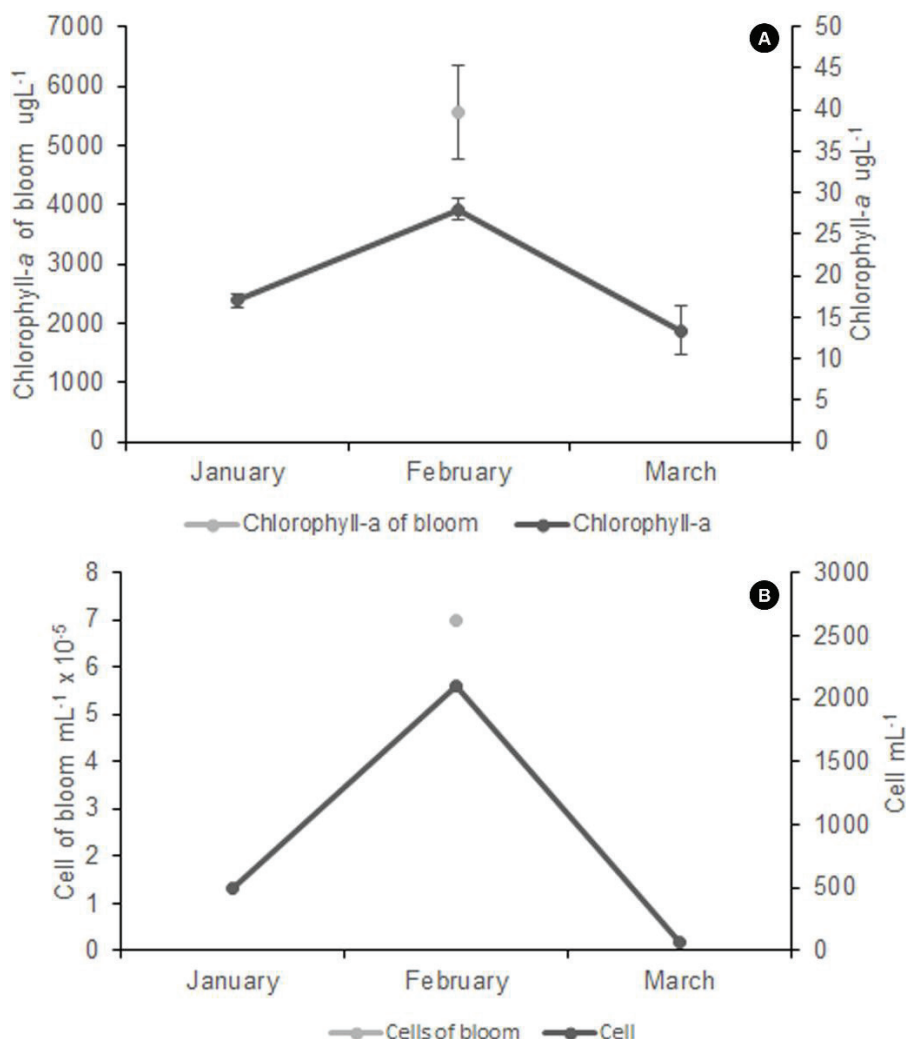


Figure 5. - Chlorophyll concentration (A) and *Chlamydomonas* cell density (B) before (January 2016), during (February 2016), and after bloom (March 2016).

severe phosphate limitation, chlorophyll synthesis is delayed but not stalled, as intracellular phosphate is sufficient to continue cell division, at least for a short time (Khozin-Goldberg & Cohen, 2006). There was a trend towards phosphorus limitation in the dry season in the NL, but total P deprivation for algae never occurred. This is proven by seeing phosphate-deprived microalgae with an increase in triacylglycerols (TAG), observed as oil droplets in the cells, which was not detected in the *Chlamydomonas* from the Cantera Oriente (Khozin-Goldberg & Cohen, 2006). The substantial imbalance found in the N:P ratio (Table 4) demonstrates physiological stress with the possibility of increased production of allelochemical compounds resulting in *Chlamydomonas* developing as a mono-specific population (Granéli *et al.*, 2008).

Ash correlates directly with the aquatic environment's concentrations of inorganic substances and salts. According to Darwish *et al.* (2020), the relatively high ash content may help explain its high pigment concentration because chlorophyll has an inorganic magnesium core.

The total carbon content of the alga is related to the carbohydrate content (Table 4, in Fig. 3C, D; Fig. 4B). During photosynthesis, phytoplankton absorbs carbon dioxide from the environment and trap solar energy, using this energy to convert inorganic carbon into carbohydrates and releasing oxygen to the environment (Reynolds, 1984; Basu & Pick, 1997; Altman & Paerl, 2012). The presence of starch is very evident in the reaction to Lugol (Fig. 2C) and in the starch halo surrounding the pyrenoids (Fig. 3C, D).

There has been much debate about the concentrations of nitrogen and phosphorus needed to cause algal blooms in water bodies. Algal response to nitrogen and phosphorus differs among aquatic ecosystems, and the development of notable phytoplankton blooms may require lower concentrations of soluble inorganic phosphorus (0.01 to 0.1 mg L⁻¹) and inorganic nitrogen (0.1 to 0.75 mg L⁻¹) (Boyd, 2015). The-

Table 5. Environmental conditions in the North Lake before (January 2016), during (February 2016), and after the algae blooming (March 2016) of *C. reinhardtii*.

Parameter	Before algae blooming	During algae blooming	After algae blooming
Temperature (° C)	12.1	14.7	17.0
pH	6.7	7.3	7.4
Bicarbonate (mg L ⁻¹)	39	34	34
Calcium (mg L ⁻¹)	37	34	32
Magnesium (mg L ⁻¹)	26	29	25
Conductivity (µS cm ⁻¹)	389	419	392
D.O. (mg L ⁻¹)	8.1	8.8	7.1
P-PO ₄ (mg L ⁻¹)	0.11	0.15	0.15
N-NH ₃ (mg L ⁻¹)	0.05	0.10	0.18
N-NO ₂ (mg L ⁻¹)	0.013	0.021	0.042
N-NO ₃ (mg L ⁻¹)	5.9	5.4	5.6

se bloom-development conditions at low phosphorus concentrations were observed in the case of the Cantera Oriente.

The linear regression model showed that chlorophyll-a concentration was positively correlated with abundance ($p < 0.001$; $r^2 = 0.94$), indicating that there seems to be a significant contribution of *Chlamydomonas* to primary production during bloom through the photosynthesis they can perform with the concentration of chlorophyll-a they contain. The values of chlorophyll-a abundance and concentration are very high, but it must be considered that the bloom occupied only a few superficial centimeters of the water column, which moderates its contribution to production.

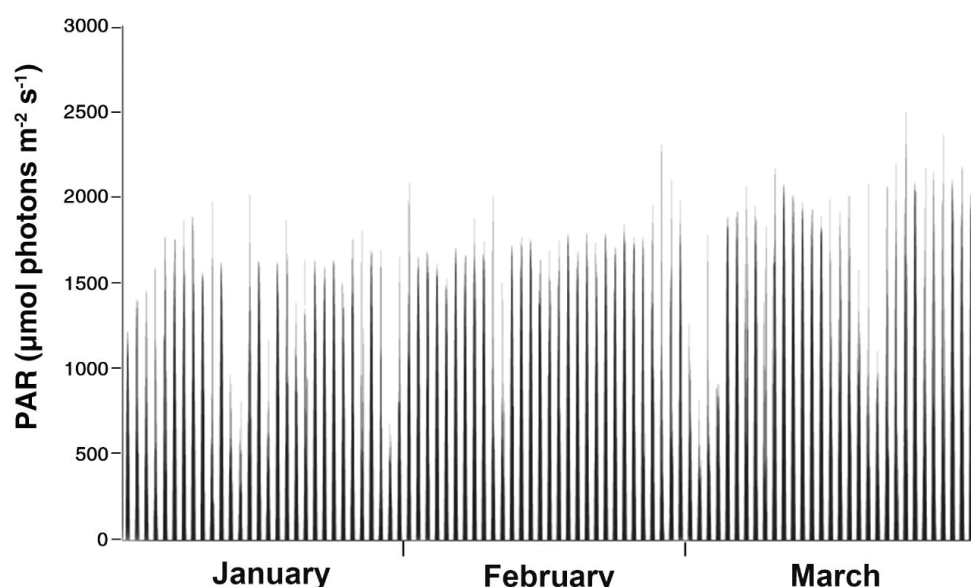


Figure 6. - Photosynthetically active radiation (PAR) before (January 2016), during (February 2016), and after bloom (March 2016).

Water quality is influenced by geological, hydrological, climatic, and anthropogenic factors (Espinal-Carreón *et al.*, 2013; Boyd, 2015); however, water temperature is considered one of the most influential parameters in water bodies (Wetzel & Likens, 2000). The *Chlamydomonas* bloom in the northern lake occurred in winter when the water temperature was slightly lower; however, Janse van Vuuren & Pieterse (2005) noted that Chlorophyceae (green algae) could occupy a more comprehensive temperature range, from below 15 °C to above 20 °C (Hixson & Arts, 2016).

It is concluded that the algal bloom consisted mainly of *Chlamydomonas reinhardtii* determined based on LM, SEM, TEM, and fluorescence studies. However, it would be essential to perform molecular studies of this Mexican species in the future. The presence of intracellular oil droplets (TAG) was not found, indicating that the alga was not in a nutrient-limited state but had active cell division. The abundance of cells in this bloom significantly correlated correlation with the chlorophyll-a concentration, indicating this alga's high photosynthetic capacity. Chemical analyses of the algae indicated low concentrations of proteins and carbohydrates, although moderate concentrations of lipids. The fatty acid composition was poor but included unsaturated fatty acids of importance in animal feed.

The lipids and fatty acids of *C. reinhardtii* are scarce compared to cultivated algae (Table 3); however, it is important to mention that this wild alga comes from natural conditions and contains a beneficial alpha-linolenic acid (omega 3), a component in the cardiovascular and neurological health of humans (Darwish *et al.*, 2020). However, further studies of this alga under controlled culture conditions (bioreactor) and its gene expression are required to use it as a biotechnological resource.

ACKNOWLEDGEMENTS

This study was supported by project PAPIIT IN221115 (DGAPA, Universidad Nacional Autónoma de México). We acknowledge the support of Francisco Martínez Pérez† and the REPSA authorities. We thank Berenit Mendoza Garfias for her assistance in the SEM process. We thank Dr. Michael Wynne for his valuable comments.

REFERENCES

AGUSTINA, S., N. N. AIDHA, E. OKTARINA & I. SETIAWATI. 2020. Antioxidant activity of *Porphyridium cruentum* water extracts for cosmetic cream. *IOP Conference Series: Materials Science and Engineering* 980: 012042. DOI:10.1088/1757-899X/980/1/012042

ALLEN, M. B. & D. I. ARNON. 1955. Studies on nitrogen-fixing blue-green algae. I. growth and nitrogen fixation by *Anabaena cylindrica* Lemm. *Plant Physiology* 30:366-372. DOI:10.1104/pp.30.4.366

ALTMAN, J.C. & H. W. PAERL. 2012. Composition of inorganic and organic nutrient sources influences phytoplankton community structure in the New River Estuary, North Carolina. *Aquatic Ecology* 46:269-282. DOI:10.1007/s10452-012-9398-8

AOAC INTERNATIONAL. 2019. *Official methods of analysis of AOAC International*, 21st ed., AOAC. Gaithersburg.

APHA, AWWA, WPCF, 1985. *Standard methods for the examination of water and wastewater*. 15th ed. APHA. Washington, DC.

ARAR, E. J. & G. B. COLLINS. 1997. *Method 445.0: In vitro determination of chlorophyll and pheophytin a in marine and freshwater algae by fluorescence*. United States Environmental Protection Agency, Office of Research and Development, National Exposure Research Laboratory.

BALDIA, S. F., M. C. G. CONACO, T. NISHIJIMA, S. IMANISHI & K. I. KARADA. 2003. Microcystin production during algal bloom occurrence in Laguna de Bay the Philippines. *Fisheries Science* 69:110-116. DOI:10.1046/j.1444-2906.2003.00594.x

BARKA A. & C. BLECKER. 2016. Microalgae as a potential source of single-cell proteins. *A review*. *Biotechnology, Agronomy, Society and Environment* 20:427-436. DOI:10.25518/1780-4507.13132

BARREIRO, A. & N.G. HAIRSTON, JR. 2013. The influence of resource limitation on the allelopathic effect of *Chlamydomonas reinhardtii* on other unicellular freshwater planktonic organisms. *Journal of Plankton Research* 35:1339-1344. DOI:10.1093/plankt/fbt080

BASU, B. K. & F. R. PICK. 1997. Phytoplankton and zooplankton development in a lowland river. *Journal of Plankton Research* 19:237-253. DOI:10.1093/plankt/19.2.237

BECKER, W. 2004. Microalgae in human and animal nutrition. In: Richmond, A. (ed.). *Handbook of microalgal culture: biotechnology and applied phycology*. Blackwell Publishing Ltd, Wiley Online Library, pp. 312-351.

BOYD, C. E. 2015. Microorganisms and water quality. In: Boyd, C.E. (ed.). *Water quality*. Springer International Publishing, Switzerland, pp. 189-222. DOI:10.1007/978-3-319-17446-4_10

CATALÁN, J. 1984. Agregados de algas en la superficie del agua (Delta del Llobregat). *Anales de Biología* 2 (Sección especial): 75-83.

CUEVAS-MADRID, H., A. LUGO-VÁZQUEZ, L. PERALTA-SORIANO, J. MORLÁN-MEJÍA, G. VILA CLARA-FATJÓ, M.R. SÁNCHEZ-RODRÍGUEZ, M.A. ESCOBAR-OLIVA & J. CARMONA-JIMÉNEZ. 2020. Identification of key factors affecting the trophic state of four tropical small water bodies. *Water* 12:1454. DOI:10.3390/w12051454

DANGEARD, P. A. 1888. Recherches sur les algues inférieures. *Annales des Sciences Naturelles: Botanique*, sér. 7, 7:105-175.

DARWISH, R., M. A. GEDI, P. AKEPACH, H. ASSAYE, A.S. ZAKY, & D. A. GRAY. 2020. *Chlamydomonas reinhardtii* is a potential food supplement with the capacity to outperform *Chlorella* and *Spirulina*. *Applied Sciences* 10(19):6736. DOI:10.3390/app10196736

DEAN, A. P., J. M. NICHOLSON, & D. C. SIGEE. 2008. Impact of phosphorus quota and growth phase on carbon allocation in *Chlamydomonas reinhardtii*: an FTIR microspectroscopy study. *European Journal of Phycology* 43:345-354. DOI:10.1080/09670260801979287

EL-BAZ, K., S. M. ABDO & A. M. S. HUSSEIN. 2017. Microalgae *Dunaliella salina* for use as food supplement to improve pasta quality. *International Journal of Pharmaceutical Sciences Review and Research* 46:45-51.

ESPINAL-CARREÓN, T., J. E. SEDEÑO, & E. LÓPEZ. 2013. Evaluación de la calidad del agua en la laguna de Yuriria, Guanajuato, México, mediante técnicas multivariadas: un análisis de valoración para dos

épocas 2005, 2009-2010. *Revista Internacional de Contaminación Ambiental* 29:147-163.

GRANÉLI, E., M. WEBERG & P. S. SALOMON. 2008. Harmful algal blooms of allelopathic microalgal species: The role of eutrophication. *Harmful Algae* 8:94-102. DOI: 10.1016/j.hal.2008.08.011

GREENSPAN, P., E. P. MAYER & S. D. FOWLER. 1985. Nile red: a selective fluorescent stain for intracellular lipid droplets. *Journal of Cell Biology* 100:965-973. DOI: 10.1083/jcb.100.3.965

GUIRY, M. D. & G. M. GUIRY. 2021. AlgaeBase. World-wide electronic publication, National University of Ireland, Galway. Available online at: <https://www.algaebase.org> (downloaded June 6 2021).

HAMMER, Ø., D. A. T. HARPER P. D. & RYAN. 2001. PAST: Paleontological Statistics Software Package for education and data analysis. *Palaeontologia Electronica* 4:9.

HEIMERL, N., E. HOMMEL, M. WESTERMANN, D. MEICHNER, M. LOHR, C. HERTWECK, A. R. GROSSMAN, M. MITTAG & S. SASSO. 2018. A giant type I polyketide synthase participates in zygospore maturation in *Chlamydomonas reinhardtii*. *The Plant Journal* 95:268-281. DOI: 10.1111/tpj.13948

HERNÁNDEZ-TORRES, A., A. L. ZAPATA-MORALES, A. E. OCHOA ALFARO & R. E. SORIA-GUERRA. 2016. Identification of gene transcripts involved in lipid biosynthesis in *Chlamydomonas reinhardtii* under nitrogen, iron, and sulphur deprivation. *World J Microbial Biotechnology* 32:55. DOI: 10.1007/s11274-016-2008-5

HERRMAN, V. & F. JÜTTNER. 1977. Excretion products of algae. Identification of biogenic amines by gas-liquid chromatography and mass spectrometry of their trifluoroacetamides. *Analytical Biochemistry* 78:365-373.

HIXON, S. M. & M. T. ARTS. 2016. Climate warming is predicted to reduce omega-3, long-chain, polyunsaturated fatty acid production in phytoplankton. *Global Change Biology* 22:2744-2755. DOI: 10.1111/gcb.13295

JANSE VAN VUUREN, S. & A. H. J. PIETERSE. 2005. The use of multivariate analysis as a tool to illustrate the influence of environmental variables on phytoplankton composition in the Vaal River, South Africa. *African Journal of Aquatic Science* 30:17-28. DOI: 10.2989/16085910509503830

JHA, P., A. K. BISWAS, B. L. LAKARIA, R. SAHA, M. SINGH & A. SUBBA RAO. 2014. Predicting total organic carbon content of soils from Walkley and Black Analysis. *Communications in Soil Science and Plant Analysis* 45:713-725. DOI: 10.1080/00103624.2013.874023

JOHN, D. M., B. A. WHITTON & A. J. BROOK (eds.). 2011. *The freshwater algal flora of the British Isles. An identification guide to freshwater and terrestrial algal*. Cambridge University Press, Cambridge, 702 pp.

KALISCH, B., P. DÖRMANN & G. HÖLZL. 2016. DGDG and Glycolipids in plants and algae. *Subcellular Biochemistry* 86:51-83. DOI: 10.1007/978-3-319-25979-6_3

KHOZIN-GOLDBERG, I. & Z. COHEN. 2006. The effect of phosphate starvation on the lipid and fatty acid composition of the fresh water eustigmatophyte *Monodus subterraneus*. *Phytochemistry* 67:696-701. DOI: 10.1016/j.phytochem.2006.01.010

KRUSKOPF, M. M. & S. DU PLESSIS. 2004. Induction of both acid and alkaline phosphatase activity in two green-algae (Chlorophyceae) in low N and P concentrations. *Hydrobiologia* 513:59-70. DOI: 10.1023/B:hydr.0000018166.15764.b0

LOT, A. (COORD.) 2007. Guía ilustrada de la Cantera Oriente. *Caracterización ambiental e inventario biológico*. Universidad Nacional Autónoma de México, México, 253 pp.

LUGO-VÁZQUEZ, A., M. R. SÁNCHEZ-RODRÍGUEZ, J. MORLÁN-MEJÍA, L. PERALTA-SORIANO, E. A. ARELLANES-JIMÉNEZ, M. A. ESCOBAR-OLIVA & M. G. OLIVA-MARTÍNEZ. 2017. Ciliates and trophic urban ponds in Mexico City. *Journal of Environmental Biology* 38 (Special issue):1161-1169. DOI: 10.22438/jeb/38/6(SI)/01

MANSILLA, M. C., L. E. CYBULSKI, D. ALBANESI & D. DE MENDOZA. 2004. Control of membrane lipid fluidity by molecular thermosensors. *Journal of Bacteriology* 186:6681-6688. DOI: 10.1128/JB.186.20.6681-6688.2004

MILLIE, D. F., C. P. DIONIGI, O. M. E. SCHOFIELD, G. T. KIRKPATRICK & P. A. TESTER. 1999. What is the importance for understanding the molecular, cellular, and ecophysiological bases of harmful algal blooms? *Journal of Phycology* 35:1353-1355.

MOELLERLING, E. R. & C. BENNING. 2010. RNA interference silencing of a major lipid droplet protein affects lipid droplet size in *Chlamydomonas reinhardtii*. *Eukaryotic Cell* 9:97-106. DOI: 10.1128/EC.00203-09

MOHAN, C. 2006. Buffers: A guide for the preparation and use of buffers in biological systems. EMD, Merck, San Diego, 32 pp.

MOWE, M. A., S. M. MITROVIC, R. P. LIM, A. FUREY & D. C. YEO. 2015. Tropical cyanobacterial blooms: a review of prevalence, problem taxa, toxins and influencing environmental factors. *Journal of Limnology* 74:205-224. DOI: 10.4081/jlimnol.2014.1005

OCHOA-ALFARO, A. E. D. E. GAYTÁN-LUNA, O. GONZÁLEZ-ORTEGA, K. G. ZAVALA-ARIAS, L. M. T. PAZ-MALDONADO, A. ROCHA-URIBE & R. E. SORIA-GUERRA. 2019. pH effects on the lipid and fatty acids accumulation in *Chlamydomonas reinhardtii*. *Biotechnology Progress* 2019:e2891. DOI: 10.1002/btpr.28

OLIVEIRA, C. Y. B., T. L. VIEGAS, M. F. OLIVEIRA DA SILVA, D. MACHADO-FRACALOSSI, R. GARCIA-LOPES & R. BIANCHINI-DERNER. 2020. Effect of trace metals on growth performance and accumulation of lipids, proteins, and carbohydrates on the green microalga *Scenedesmus obliquus*. *Aquaculture International* 28:1435-1444. DOI: 10.1007/s10499-020-00533-0

PASCHER, A. VON. 1927. Volvocales Phytomonadinae Flagellate I- Chlorophyceae I. In: Pascher, A. (ed.). *Die Süßwasserflora Deutschlands, Österreichs Und Der Schweiz. Herausgegeben*. Gustav Fischer, Jena, No. 4.

PEHRSSON, P., K. PATTERSON, D. HAYTOWITZ & K. PHILLIPS. 2015. Total carbohydrate determinations in USDA's National Nutrient Database for Standard Reference. *The Federation of American Societies for Experimental Biology Journal* 29:740-746. DOI: 10.1096/fasebj.29.1_supplement.740.6

PIETERSE, A. J. H. & S. JANSE VAN VUUREN. 1997. *An investigation into phytoplankton blooms in the Vaal River and the environmental variables responsible for their development and decline*. Report to the Water

Research Commission by the Department of Plant and Soil Sciences. Potchefstroom University for CHE. Water Research Commission (SA) Report, 359/1/97.

PRÖSCHOLD, T., T. DARIENKO, L. KRIENITZ & A. W. COLEMAN. 2018. *Chlamydomonas schloesseri* sp. nov. (Chlamydophyceae, Chlorophyta) revealed by morphology, autolysin cross experiments, and multiple gene analyses. *Phytotaxa* 362:21-38. DOI:10.11646/phytotaxa.362.1.2

REYNOLDS, C. S. 1984. *Ecology of phytoplankton*. Cambridge University Press, Cambridge, 384 pp.

RIVER SCIENCE. 2005. *Algal blooms in the Swan-Canning estuary: patterns, causes and history*. Government of Western Australia Issue 3, 12 pp. <https://www.dpaw.wa.gov.au/images/documents/conservation-management/riverpark/fact-sheets/River%20Science%203%20-%20Algal%20Blooms.pdf>

SALAS-MONTANTES, C. J., O. GONZÁLEZ-ORTEGA, A. E. OCHOA-ALFARO, R. CAMARENA-RANGEL, L. M. T. PAZ-MALDONADO, S. ROSALES-MENDOZA, A. ROCHA-URIBE & R. E. SORIA-GUERRA. 2018. Lipid accumulation during nitrogen and sulfur starvation in *Chlamydomonas reinhardtii* overexpressing a transcription factor. *Journal of Applied Phycology* 30:1721-1733. DOI: 10.1007/s10811-018-1393-6

SCRANTON, M. A., J. T. OSTRAND, F. J. FIELDS & S. P. MAYFIELD. 2015. *Chlamydomonas* as a model for biofuels and bio-products production. *The Plant Journal* 82:523-531. DOI:10.1111/tpj.12780

SIAUT, M., S. CUINÉ, C. CAGNON, B. FESSLER, M. NGUYEN, P. CARRIER, A. BEYLY, F. BEISSON, C. TRIANTAPHYLIDES, Y. LI-BEISSON & G. PELTIER. 2011. Oil accumulation in the model green alga *Chlamydomonas reinhardtii*: characterization, variability between common laboratory strains and relationship with starch reserves. *BMC Biotechnology* 11:7. <http://www.biomedcentral.com/1472-6750/11/7>

SMITH, D. R., H. P. JARVIE & M. J. BOWES. 2017. Carbon, nitrogen, and phosphorus stoichiometry and eutrophication in River Thames Tributaries, UK. *Agricultural & Environmental Letters* 2:170020. DOI:10.2134/ael2017.06.0020

TOLEDO, J., M. ESTEVE, M. GRASA, A. LEDDA, H. GARDAC, J. GULFO, I. DÍAZ LUDOVICO, N. RAMELLA & M. GONZALEZ. 2016. Data related to inflammation and cholesterol deposition triggered by macrophages exposition to modified LDL. *Data in Brief* 8:251-257.

VALDERRAMA, J. C. 1981. The simultaneous analysis of total nitrogen and total phosphorus in natural waters. *Marine Chemistry* 10:109-122.

WETZEL, R. G. & G. E. LIKENS. 2000. *Limnological analyses*. Springer Verlag, New York, 419 pp.